JOURNAL OF AEROSOL MEDICINE AND PULMONARY DRUG DELIVERY
Volume 35, Number 6, 2022
Mary Ann Liebert, Inc.
Pp. 296–306
DOI: 10.1089/jamp.2022.0043

Open camera or QR reader and scan code to access this article and other resources online.

Comparison of Dose–Response Relationships for Two Isolates of SARS-CoV-2 in a Nonhuman Primate Model of Inhalational COVID-19

Paul A. Dabisch, PhD,[*,1] Jaleal S. Sanjak, PhD,[2] Jeremy A. Boydston, MS,[1] John Yeager, BS,[1] Artemas Herzog, MS,[3] Jennifer Biryukov, PhD,[1] Katie Beck, BS,[1] Danh Do, PhD,[1] Brittany G. Seman, PhD,[1] Brian Green, MS,[1] Jordan K. Bohannon, MS,[1] Brian Holland, BS,[1] David Miller, MS,[1] Taylor Ammons, BS,[1] Denise Freeburger, BS,[1] Susan Miller, BS,[1] Tammy Jenkins,[1] Sherry Rippeon,[1] James Miller,[1] David Clarke,[1] Emmanuel Manan,[1] Ashley Patty,[1] Kim Rhodes,[1] Tina Sweeney,[1] Michael Winpigler,[1] Louis A. Altamura, PhD,[1] Heather Zimmerman, DVM,[1] Alec S. Hail, DVM,[1] Victoria Wahl, PhD,[1] and Michael Hevey, PhD[1]

Abstract

Background: As the COVID-19 pandemic has progressed, numerous variants of SARS-CoV-2 have arisen, with several displaying increased transmissibility.
Methods: The present study compared dose–response relationships and disease presentation in nonhuman primates infected with aerosols containing an isolate of the Gamma variant of SARS-CoV-2 to the results of our previous study with the earlier WA-1 isolate of SARS-CoV-2.
Results: Disease in Gamma-infected animals was mild, characterized by dose-dependent fever and oronasal shedding of virus. Differences were observed in shedding in the upper respiratory tract between Gamma- and WA-1-infected animals that have the potential to influence disease transmission. Specifically, the estimated median doses for shedding of viral RNA or infectious virus in nasal swabs were approximately 10-fold lower for the Gamma variant than the WA-1 isolate. Given that the median doses for fever were similar, this suggests that there is a greater difference between the median doses for viral shedding and fever for Gamma than for WA-1 and potentially an increased range of doses for Gamma over which asymptomatic shedding and disease transmission are possible.
Conclusions: These results complement those of previous studies, which suggested that differences in exposure dose may help to explain the range of clinical disease presentations observed in individuals with COVID-19, highlighting the importance of public health measures designed to limit exposure dose, such as masking and social distancing. The dose–response data provided by this study are important to inform disease transmission and hazard modeling, as well as to inform dose selection in future studies examining the efficacy of therapeutics and vaccines in animal models of inhalational COVID-19.

Keywords: COVID-19, nonhuman primates, inhalation, dose–response, aerosol, transmission

[1]National Biodefense Analysis and Countermeasures Center, Operated by Battelle National Biodefense Institute, U.S. Department of Homeland Security, Frederick, Maryland, USA.
[2]Division of Preclinical Innovation, National Center for Advancing Translational Sciences, National Institutes of Health, Rockville, Maryland, USA.
[3]Censeo Insight, Seattle, Washington, USA.
*Member of ISAM.

Introduction

Numerous studies have detected infectious SARS-CoV-2 or viral RNA in air samples collected in the vicinity of infected individuals,[1–10] suggesting that respiratory aerosols play a role in transmission of COVID-19. As the pandemic has progressed, numerous variants of SARS-CoV-2 have emerged, with several displaying increased transmissibility.[11–15] Several studies have hypothesized that increased viral shedding from infected individuals may be an important factor associated with the increased transmissibility observed with more recent variants of SARS-CoV-2.[3,13,16–19] Other potential explanations include enhanced survival of virus during transport through the environment, and/or a lower infectious dose in susceptible individuals, although the relative contributions of these potential mechanisms remain unclear.

A recent study from our laboratory found that the probability of infection following inhalation of an early isolate of SARS-CoV-2, hCoV-19/USA/WA-1/2020 (WA-1), was dose dependent in a nonhuman primate (NHP) model of inhalational COVID-19. Furthermore, the median dose necessary to elicit an immune response was significantly lower than that needed to cause fever, suggesting that exposure dose may be a factor influencing disease presentation.[20] These results are in agreement with several other studies that have similarly demonstrated dose dependence of disease presentation in rodent models of COVID-19.[21,22] However, no studies were identified, which compared dose–infectivity relationships for different variants of SARS-CoV-2.

To assess whether changes in the infectious dose or viral shedding contribute to the increased transmissibility associated with more recent variants of SARS-CoV-2, the present study compared dose–response relationships and disease presentation in NHPs infected with an isolate of the Gamma variant of SARS-CoV-2, which has multiple mutations in the S protein, which have been shown to contribute to increased viral fitness,[23–25] to the results of our previous study with the earlier WA-1 isolate.

Materials and Methods

Ethics statement

All research was conducted in compliance with the Animal Welfare Act and other federal statutes and regulations relating to animals and experiments involving animals and adheres to principles stated in the *Guide for the Care and Use of Laboratory Animals*,[26] and was conducted in accordance with a Protocol approved by both the National Biodefense Analysis and Countermeasures Center Institutional Animal Care and Use Committee and the U.S. Department of Homeland Security Compliance and Assurance Program Office. The facility where this research was conducted is fully accredited by the Association for Assessment and Accreditation of Laboratory Animal Care International and maintains a Public Health Service Humane Care and Use of Laboratory Animals Policy assurance. All work was conducted in accredited Biosafety Level 3 (BSL-3)/Animal Biosafety Level 3 (ABSL-3) laboratories.

Virus

An isolate of SARS-CoV-2 Gamma (hCoV-19/Japan/TY7-503/2021; NR-54984, Lot#70043069, BEI Resources; GISAID: EPI_ISL_792683) was provided by National Institute of Allergy and Infectious Diseases (NIAID) and was stored at −80°C until use. The Gamma variant contains numerous mutations in the S protein relative to the WA-1 isolate, some of which have been shown to result in changes in binding affinity and viral replication that potentially contribute to increased viral fitness.[23–25] Additional details on this isolate are provided in the Supplementary Data.

Animals

Previous studies have demonstrated that cynomolgus macaques are susceptible to infection with aerosolized SARS-CoV-2 through inhalation, including a previous study from our laboratory that reported dose–response relationships for the earlier WA-1 isolate of SARS-CoV-2.[20,27,28] Therefore, in the present study, 21 healthy, adult cynomolgus macaques (*Macaca fascicularis*; 10 male and 11 female; 4–8 years old; NIH Animal Center, Poolesville, MD), weighing 2.9–6.5 kg at the time of exposure, were utilized to assess dose–response relationships for SARS-CoV-2 Gamma for comparison to our previously reported data with the WA-1 isolate. All animals were serologically naive for SARS-CoV-2 before study as measured using the Euroimmun SARS-CoV-2 S1 ELISA Kit (El 2606-9601 G; Euroimmun Inc.) and negative by reverse transcription–real-time PCR (RT-qPCR) in nasal swabs. Animals were housed in high efficiency particulate air (HEPA)-filtered isolator cages (37324; Carter$_2$ Systems, Inc.) throughout the study to minimize the potential for disease transmission among animals housed in the same room. The mean (±standard deviation) relative humidity and temperature in the housing room over the course of the study were $50.8 \pm 2.9\%$ and 23.9 ± 0.7°C, respectively.

Inhalation exposures

Inhalation exposures were conducted identically to those performed as part of our previous study with the WA-1 isolate.[20] The number median aerodynamic diameter of the generated aerosols was 0.78 ± 0.01 μm with a geometric standard deviation (GSD) of 1.44 ± 0.02, similar to the size distribution reported previously for particles exhaled from the human respiratory tract during breathing.[29] The corresponding mass median aerodynamic diameter was 1.51 ± 0.08 μm with a GSD of 1.56 ± 0.02. Additional details on the exposure methodology, as well as a summary of exposure parameters and doses for each animal are included in the Supplementary Data.

Three groups of 6–8 animals were exposed iteratively to aerosolized SARS-CoV-2. Doses for the initial iteration were based on the results of our previous study with the WA-1 isolate. The results from each iteration were utilized to inform dose selection for the subsequent iteration, with the goal of minimizing the confidence interval for the median doses.

Postexposure observations and sample collection

Animals were observed twice daily for clinical signs of illness for 21 days postexposure. Body temperature was monitored continuously utilizing implanted telemetry transmitters (M00; Data Sciences International). An average daily temperature profile (15-minute resolution) for each animal was calculated based on at least 3 days of temperature data from the preexposure period. During the postexposure period,

Table 1. Comparison of Fever Metrics for Animals Exposed to SARS-CoV-2 Gamma and WA-1

Metric	*Gamma*	*WA-1*	p
Median deposited dose for fever, in $\log_{10}$ $TCID_{50}$ (95% CI)	2.0 (1.4–2.7)	2.4 (1.9–3.3)	0.19
Median time to fever onset, in hours (range)	34.3 (29.0–61.0)	34.0 (17.8–41.3)	0.33
Median duration of fever, in hours (range)	4.6 (2.3–9.3)	5.5 (2.5–12.8)	0.35
Number of NHPs with fever	6	5	NA

Median doses for fever were compared through LRT, while the median times for fever onset and fever duration were compared through unpaired *t*-tests.

CI, confidence interval; LRT, likelihood ratio test; NA, not applicable; NHPs, nonhuman primates; $TCID_{50}$, median tissue culture infectious doses.

fever was defined as an increase of 1°C above the time-matched average from the preexposure period for ≥2 hours.

Animals were anesthetized (Telazol; 3 mg/kg i.m.) on days 2, 4, 6, 8, 10, 14, and 21 postexposure for collection of blood/serum samples, nasopharyngeal and oropharyngeal swabs, and exhaled breath samples.

Serum samples were utilized to assess seroconversion using a plaque reduction neutralization test (PRNT) and serum chemistries, as described previously[20] and in the Supplementary Data.

Nasopharyngeal and oropharyngeal samples were collected using sterile specimen collection swabs (VF105-80; Vare Health), placed into 15-mL conical tubes containing 3 mL of viral culture medium, and vortexed for ~5 seconds. For nasopharyngeal swabs, both nares were swabbed using a single swab. Samples were then assayed for infectious virus by microtitration or for the presence of viral RNA using RT-qPCR (see Supplementary Data for details).

Exhaled breath collection utilized an anesthesia mask (Surgivet mask 32393B1; Patterson Veterinary) supplied with HEPA-filtered, dry (relative humidity <10%), compressed air. The mask exhaust airflow was sampled using an Optical Particle Sizer (OPS) (1 L/min; Model 3330, TSI Inc.), and a polytetrafluoroethylene (PTFE) Filter (5 L/min). At the end of the collection period, PTFE filters were resuspended in minimum essential medium for growth (gMEM) and analyzed by microtitration and RT-qPCR. A schematic of the system and additional details on the exhaled breath collection system are provided in the Supplementary Data.

Data analysis

Dose–response relationships for viral shedding, fever, and seroconversion were modeled separately using a univariate GLM approach, with data for each endpoint used to construct a binary variable that reflected whether a subject was positive for the endpoint of interest at any point during the postexposure observation period. Binary data were fit with a probit dose–response model with viral variant treated as a covariate (JMP 16.1; SAS Institute, Inc.). Bivariate analyses similar to those utilized in our previous study were also performed.[20] Other comparisons were performed using Prism (v. 9.2.0; GraphPad Software LLC.). The specific analyses performed for each comparison are detailed in the Results section.

Results

Six of the 21 animals exposed to SARS-CoV-2 Gamma developed transient periods of fever postexposure (Table 1). The median deposited dose for development of fever, as well as the median time to fever onset and median fever duration were similar to those observed in our previous study with WA-1 (Tables 1 and 2). The results of probit analysis suggest that viral variant is not a significant factor influencing the dose–response relationships for fever ($p = 0.19$ through likelihood ratio test [LRT]). Temperature profiles are shown in Figure 1 and in the Supplementary Data. Gamma-infected animals with fever also displayed a transient lymphopenia that resolved by 4 days postexposure,

Table 2. Comparison of Median Doses for Fever, Shedding, and Development of Neutralizing Titers

Isolate/ variant	*Median dose for indicated endpoint*			
	$PRNT_{50}$ >10	*Shedding in nasopharyngeal swabs*		*Fever*
WA-1	1.2 $\log_{10}$ $TCID_{50}$ (85% CI: 0.6 to 1.6)	Viral RNA	1.9 $\log_{10}$ $TCID_{50}$ (85% CI: 1.4 to 2.5)	2.4 $\log_{10}$ $TCID_{50}$ (85% CI: 2.1 to 2.9)
		Infectious virus	2.6 $\log_{10}$ $TCID_{50}$ (85% CI: 2.0 to 3.3)	
Gamma	0.0 $\log_{10}$ $TCID_{50}$ (85% CI: –0.6 to 0.5)	Viral RNA	0.7 $\log_{10}$ $TCID_{50}$ (85% CI: 0.0 to 1.3)	2.0 $\log_{10}$ $TCID_{50}$ (85% CI: 1.6 to 2.4)
		Infectious virus	0.9 $\log_{10}$ $TCID_{50}$ (85% CI: 0.3 to 1.5)	

Median doses for each endpoint are presented with 85% CIs, as comparison of their overlap has been shown to be a reliable indicator of significance for independent dose–response models. Probit fits were also compared through LRT.

PRNT, plaque reduction neutralization test.

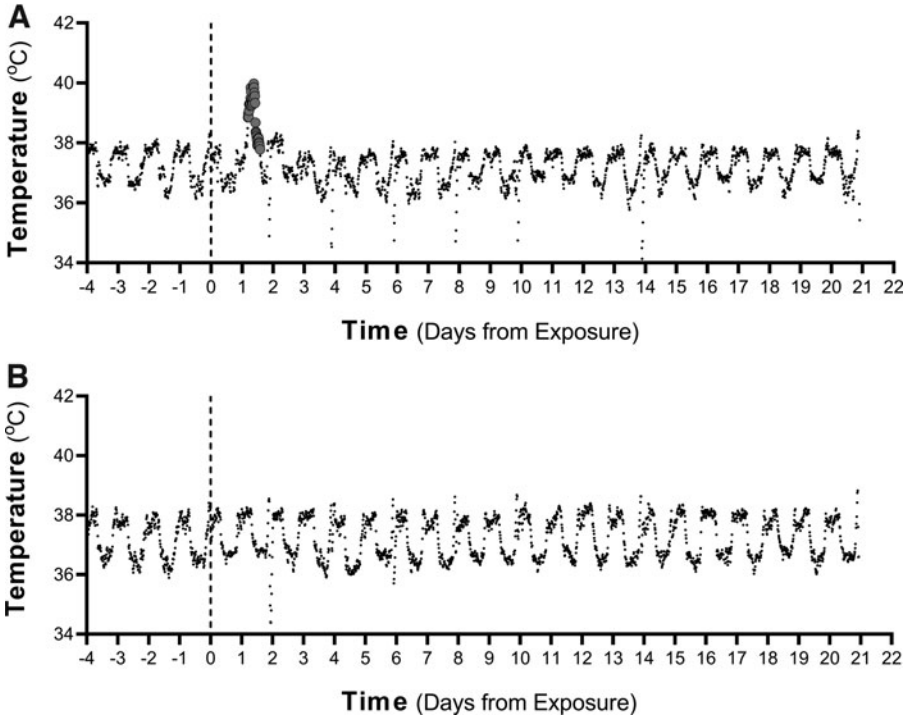

FIG. 1. Representative temperature profiles. Temperature profiles are shown for an animal, which developed a transient fever at 29 hours postexposure **(A)**, and for an animal that did not develop fever postexposure **(B)**. The deposited doses for **(A)** and **(B)** were 637.3 $TCID_{50}$ (2.80 $\log_{10}$ $TCID_{50}$) and 90.4 $TCID_{50}$ (1.96 $\log_{10}$ $TCID_{50}$), respectively. The dips in temperature observable postexposure coincide with administration of anesthesia before blood collection. $TCID_{50}$, median tissue culture infectious doses.

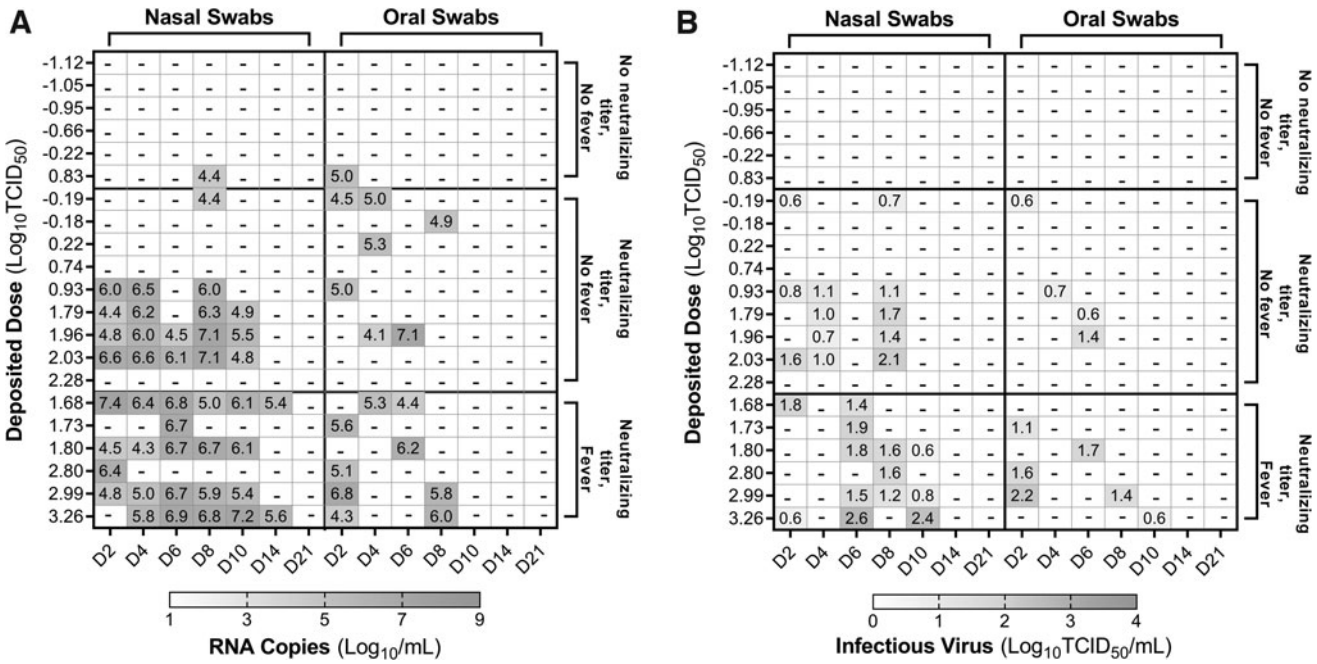

FIG. 2. Shedding of viral RNA and infectious virus in nasal and oral swabs from animals exposed to SARS-CoV-2 Gamma. Levels of viral RNA **(A)** and infectious virus **(B)** in swab samples, expressed as $\log_{10}$ RNA copies/mL and $\log_{10}$ $TCID_{50}$/mL, respectively, are shown for animals exposed to SARS-CoV-2 Gamma. Animals are grouped by disease presentation, specifically those with fever and a neutralizing titer (i.e., positive $PRNT_{50}$), those with seroconversion but without fever, and those with neither response. PRNT, plaque reduction neutralization test.

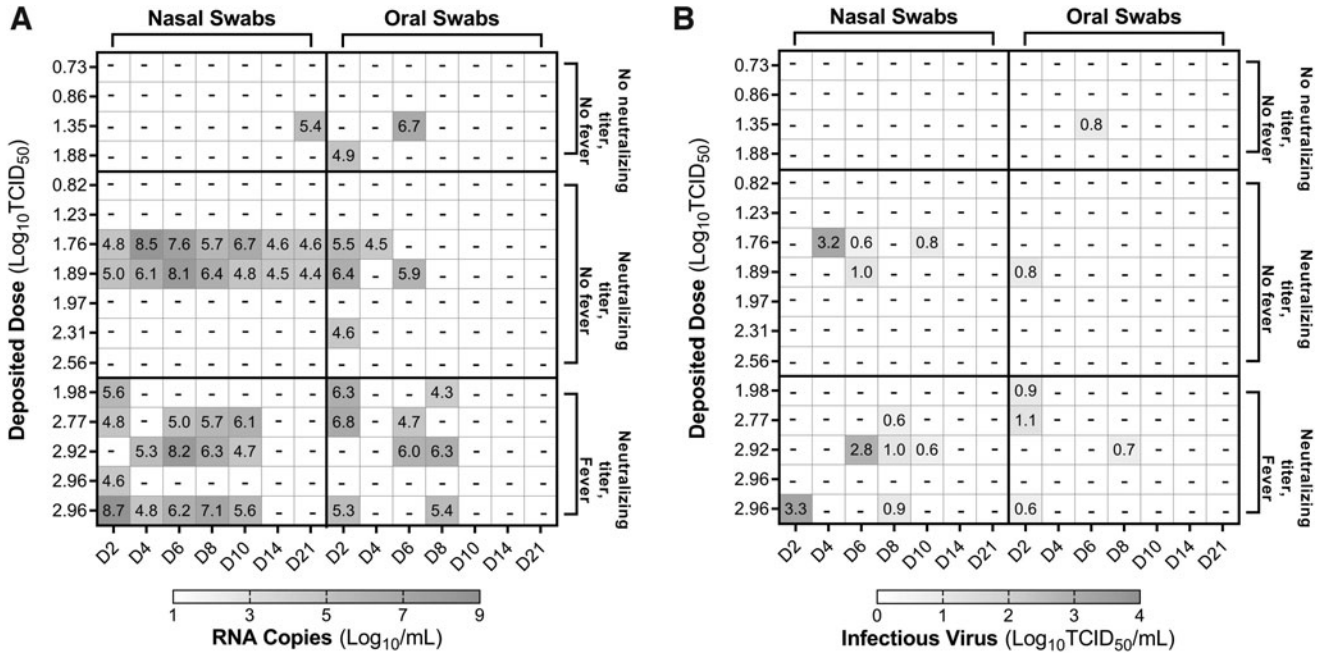

FIG. 3. Shedding of viral RNA and infectious virus in nasal and oral swabs from animals exposed to SARS-CoV-2 WA-1. Levels of viral RNA **(A)** and infectious virus **(B)** in swab samples, expressed as $\log_{10}$ RNA copies/mL and $\log_{10}$ $TCID_{50}$/mL, respectively, are shown for animals exposed to SARS-CoV-2 WA-1. Animals are grouped by disease presentation, specifically those with fever and a neutralizing titer (i.e., positive $PRNT_{50}$), those with seroconversion but without fever, and those with neither response.

as well as a borderline increase in interleukin-6 (IL-6) (Supplementary Data).

Viral RNA and/or infectious virus was detected intermittently in swabs from 14/21 Gamma-exposed animals, including all six that developed fevers (Fig. 2), and in swabs from 10/16 WA-1-exposed animals, including all five that developed fevers (Fig. 3). The results of probit analysis suggest that viral variant is a significant factor influencing the dose–response relationships for shedding of viral RNA ($p = 0.03$ through LRT) and infectious virus ($p = 0.004$ through LRT) in nasal swabs. The median dose for shedding of viral RNA or infectious virus in nasal swabs was significantly lower for the Gamma variant than for the WA-1 isolate, when assessed by overlap of 85% confidence intervals, which has been shown to be a reliable indicator of significance for independent dose–response models (Table 2).[30] While shedding occurred at lower doses for Gamma relative to WA-1, neither the peak levels nor total amount of infectious virus or viral RNA detected in swabs during the postexposure observation period were greater for Gamma relative to WA-1 ($p > 0.19$; Table 3).

The median times to peak shedding of infectious virus or viral RNA in swabs were also similar for Gamma and WA-1 ($p > 0.40$; Table 3). Finally, the median number of days on which infectious virus or viral RNA was detected in swabs postexposure were similar for Gamma and WA-1 ($p > 0.99$; Table 3).

Table 3. Comparison of Viral Shedding Metrics for Animals Exposed to SARS-CoV-2 Gamma and WA-1

Metric	*Gamma*	*WA-1*	p
Mean peak level of infectious virus detected	1.7 ± 0.5 $\log_{10}$ $TCID_{50}$/mL	2.2 ± 1.3 $\log_{10}$ $TCID_{50}$/mL	0.25
Median time to peak shedding of infectious virus	6 days (range: 2–8 days)	6 days (range: 2–8 days)	0.79
Mean total infectious virus detected postexposure	2.3 ± 0.5 $\log_{10}$ $TCID_{50}$/mL	2.7 ± 1.3 $\log_{10}$ $TCID_{50}$/mL	0.39
Median number of days of detectable shedding of infectious virus	2 days (range: 1–3 days)	2 days (range: 1–3 days)	>0.99
Mean peak level of viral RNA detected	6.4 ± 1.0 $\log_{10}$ RNA copies/mL	6.9 ± 1.6 $\log_{10}$ RNA copies/mL	0.41
Median time to peak shedding of viral RNA	7 days (range: 2–10 days)	5 days (range: 2–21 days)	0.40
Mean total viral RNA detected postexposure	7.0 ± 1.1 $\log_{10}$ RNA copies/mL	7.4 ± 1.6 $\log_{10}$ RNA copies/mL	0.54
Median number of days of detectable shedding of viral RNA	4.5 days (range: 1–6 days)	4.5 days (range: 1–7 days)	>0.99

Mean values compared using unpaired *t*-tests; Median values were compared using a Kruskal–Wallis test with a Dunn's multiple comparison's posttest.

Table 4. Summary of Fever and Plaque Reduction Neutralization Test$_{50}$ Results for Animals Exposed to SARS-CoV-2 Gamma

Deposited dose					
$TCID_{50}$	log_{10} $TCID_{50}$	Fever (yes/no)	Time to fever (HPE)	$PRNT_{50}$ (yes/no)	Day 21 $PNRT_{50}$ titer
0.1	−1.12	No	—	No	—
0.1	−1.05	No	—	No	—
0.1	−0.95	No	—	No	—
0.2	−0.66	No	—	No	—
0.6	−0.22	No	—	No	—
0.6	−0.19	No	—	Yes	160
0.7	−0.18	No	—	Yes	160
1.7	0.22	No	—	Yes	20
5.5	0.74	No	—	Yes	40
6.7	0.83	No	—	No	—
8.4	0.93	No	—	Yes	40
48	1.68	Yes	34.3	Yes	320
54	1.73	Yes	38.0	Yes	1280
62	1.79	No	—	Yes	640
63	1.80	Yes	61.0	Yes	1280
90	1.96	No	—	Yes	160
107	2.03	No	—	Yes	1280
191	2.28	No	—	Yes	640
637	2.80	Yes	29.0	Yes	160
975	2.99	Yes	34.3	Yes	640
1830	3.26	Yes	33.8	Yes	160

—, denotes not applicable; HPE, hours postexposure.

Table 5. Summary of Fever and Plaque Reduction Neutralization Test$_{50}$ Results for Animals Exposed to SARS-CoV-2 WA-1

Deposited dose					
$TCID_{50}$	log_{10} $TCID_{50}$	Fever (yes/no)	Time to fever (HPE)	$PRNT_{50}$ (yes/no)	Day 21 $PNRT_{50}$ titer
5	0.73	No	—	No	—
7	0.82	No	—	Yes	>40
7	0.86	No	—	No	—
17	1.23	ND	—	Yes	>40
22	1.35	No	—	No	—
58	1.76	No	—	Yes	320
77	1.88	No	—	No	—
78	1.89	No	—	Yes	640
93	1.97	No	—	Yes	80
96	1.98	Yes	36	Yes	640
206	2.31	No	—	Yes	160
366	2.56	No	—	Yes	640
582	2.77	Yes	17.75	Yes	320
825	2.92	Yes	41.25	Yes	80
904	2.96	Yes	30.25	Yes	640
906	2.96	Yes	34	Yes	160

Data partially reproduced from Dabisch et al.[20]
ND, no data due to malfunctioning telemetry device.

On day 21 postexposure, 15 of 21 animals exposed to SARS-CoV-2 Gamma had detectable neutralizing titers against the Gamma isolate by PRNT (Table 4). In animals exposed to SARS-CoV-2 WA-1, 12 of 16 had measurable neutralizing titers against WA-1 on day 21 postexposure (Table 5). Probit analysis suggests that viral variant is a significant factor influencing the dose–response relationships for seroconversion ($p=0.033$ through LRT). Similarly, the median dose for development of a neutralizing titer was significantly lower for Gamma relative to WA-1 when overlap of 85% confidence intervals was assessed (Table 2).

For exhaled breath measurements, the median baseline particle emission rate from all anesthetized animals was 5.6 particles/min, with an interquartile range of 1.4–21.2 particles/min ($n=37$). Occasional events, such as a sneezes or movement of mouth, produced higher numbers of particles that were detectable in the system, demonstrating that the system is capable of detecting higher concentrations (Fig. 4). Most exhaled particles measured during quiet breathing had diameters <2 μm, although occasional particles as large as 8 μm were detected.

Viral RNA was detected on filters sampling the exhaled breath at a single postexposure time point in four animals exposed to the Gamma variant, with estimated emission rates ranging from 4.7 to 5.0 $\log_{10}$ RNA copies per minute (Supplementary Data). No infectious virus was detected in the exhaled breath at any time point postexposure. Three of these animals shed viral RNA in the exhaled breath on day 2 postexposure, and viral RNA was also detected in the oral swab on the same day. Viral RNA was detected in the exhaled breath of the final animal on day 6 postexposure, but no viral RNA was detected in swabs on the same day. The particle emission rates measured in these four animals with the OPS did not significantly change over the postexposure period ($p=0.97$ using a Kruskal–Wallis test and a Dunn's multiple comparisons posttest; Fig. 5), and were similar to those measured in NHPs that did not develop signs of infection ($p=0.41$). Similarly, no changes were observed in the postexposure particle emission rates if the analysis was restricted to animals with fever ($p=0.79$; $n=6$) or animals that developed neutralizing titers ($p=0.31$; $n=15$). As with the baseline period, most exhaled particles had diameters <2 μm.

A previous study suggested a relationship between exhaled particle count and viral RNA load in nasal swabs of infected NHPs.[31] In the present study, a similar relationship was not observed between exhaled particle counts and the viral RNA load detected in temporally paired nasal swab samples across all animals ($r^2=0.008$; $n=39$ samples; Fig. 6). Similarly, no relationship was observed if this analysis is restricted only to samples from animals exposed to higher doses that developed transient fevers ($r^2=0.008$; $n=21$ samples; Fig. 6).

For animals exposed to the WA-1 isolate, viral RNA was detected on a filter sampling the exhaled breath in one animal at a single time point 14 days postexposure, with an estimated viral RNA emission rate of 4.8 $\log_{10}$ RNA copies per minute. No viral RNA was detected in swabs from the same day on which viral RNA was detected in the exhaled breath, although significant levels were found in swabs on other days [Fig. 3; Dose: 2.77 $\log_{10}$ median tissue culture infectious doses ($TCID_{50}$)]. No infectious virus was detected in the exhaled breath at any time point postexposure. Similar to Gamma-infected animals, no changes were observed in postexposure particle emission rates in animals that developed fever ($p=0.9286$; $n=5$) or in animals that developed neutralizing antibody titers ($p=0.8208$; $n=12$) following exposure to the WA-1 isolate. Most particles exhaled by WA-1-infected animals had diameters less than 3 μm, although occasional particles with diameters as large as 8 μm were detected.

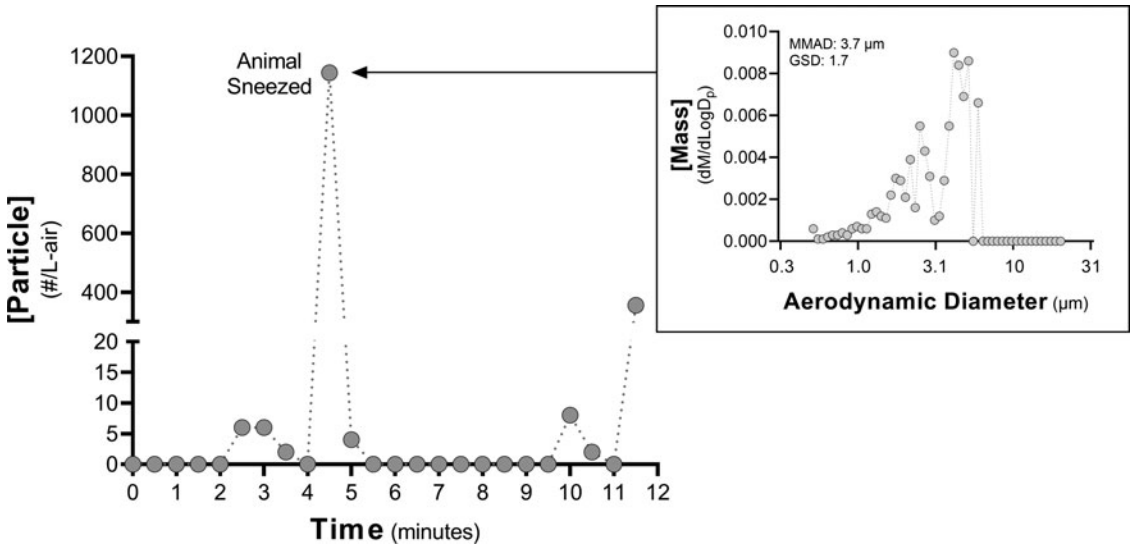

FIG. 4. Exhaled particle concentration profile and particle size distribution. The particle concentration profile during a single collection period is shown. Particle concentrations were low for the majority of the recording period. However, the animal sneezed ~3.5 minutes into the collection period, resulting in a large spike in particle concentration. The particle size distribution associated with the sneeze measured by an APS is also shown. Unfortunately, this event occurred during the preexposure period, and so no virus was detected. However, these data provide confidence that higher particle emission rates are able to be detected in the system. APS, aerodynamic particle sizer.

Discussion

The present study demonstrates that the median deposited doses for viral shedding in nasal swabs were approximately 10-fold lower for an isolate of the Gamma variant of SARS-CoV-2 than the earlier WA-1 isolate. Given that the median deposited doses for fever were similar, this suggests that there is a greater difference between the median doses for viral shedding and fever for Gamma than for WA-1 and potentially an increased range of doses for Gamma over which asymptomatic shedding and disease transmission are possible. These results also complement those of previous studies, which suggested that differences in exposure dose may help to explain the range of clinical disease presentations observed in individuals with COVID-19,[20,32,33] highlighting the importance of public health measures designed to limit exposure dose, such as masking and social distancing.

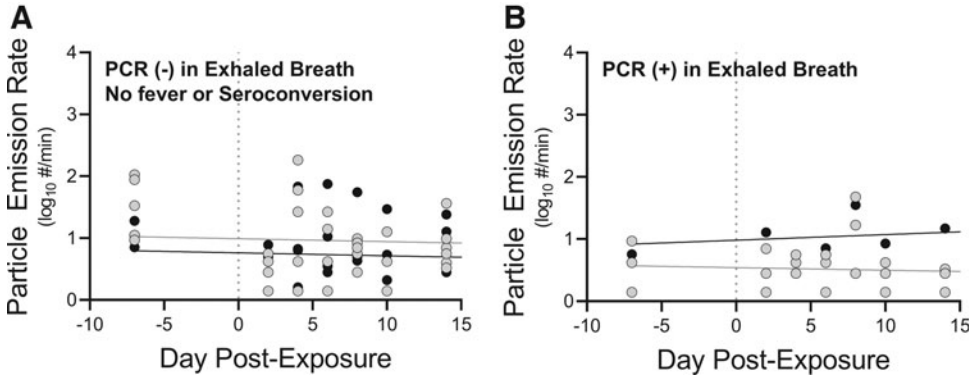

FIG. 5. Exhaled particle emission rates. **(A)** Exhaled particle emission rates are shown for uninfected animals that did not seroconvert, develop fever, or shed viral RNA in the exhaled breath. Emission rates for animals exposed to SARS-CoV-2 Gamma (gray circles) and WA-1 (black circles) are shown. **(B)** Exhaled particle emission rates are shown for animals with PCR-positive exhaled breath samples. Emission rates for the four animals infected with Gamma (gray circles) and the one animal infected with WA-1 (black circles) are shown. For animals infected with Gamma, the particle emission rates did not significantly change over the postexposure period ($p = 0.9669$) when compared using a Friedman test with Dunn's multiple comparisons posttest. Similarly, the particle emission rates were not different at any time point postexposure between uninfected animals **(A)** and those with PCR-positive exhaled breath samples **(B)** ($p = 0.41$ when compared using a Kruskal–Wallis test).

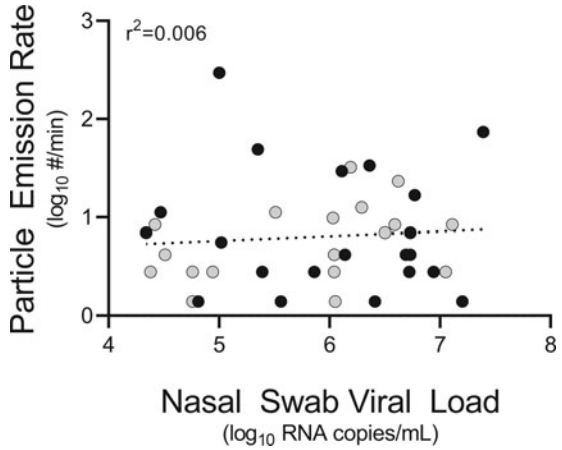

FIG. 6. Exhaled particle emission rates as a function of viral RNA load in nasal swabs for animals infected with SARS-CoV-2 Gamma. No relationship was observed between exhaled particle counts and the viral RNA load detected in nasal swab samples across all animals (black and gray circles; $r^2 = 0.006$; $n = 39$ samples). Similarly, no relationship is observed if this analysis is restricted only to samples from animals with fever (black circles; $r^2 = 0.008$; $n = 21$ samples).

The disease presentation in Gamma-infected animals was mild and consistent with previous studies that have examined the disease course following inhalation of aerosolized SARS-CoV-2.[20,27,34] Animals exposed to higher doses of Gamma developed a transient fever, with an onset between 1- and 3-day postexposure, which resolved within hours of onset. Gamma-infected animals with fever also displayed a transient increase in the IL-6 levels, and a transient lymphopenia that resolved by 4-day postexposure. While IL-6 and lymphopenia have previously been reported to correlate with disease severity in hospitalized COVID-19 patients,[35,36] the transient nature of the responses in the present study are suggestive of mild disease. No other changes were observed in parameters reported to correlate with disease severity, including neutrophils, neutrophil-lymphocyte ratio (NLR), blood urea nitrogen (BUN), creatinine, prothrombin time (PT), and activated partial thromboplastin time (aPTT),[37–39] again suggestive of mild disease.

While the dose of Gamma required to induce viral shedding in the upper respiratory tract was lower than that of WA-1, the amounts of RNA and infectious virus detected in swabs were similar for both variants. This is similar to another study in NHPs, which compared disease presentation following intranasal infection with different variants of SARS-CoV-2.[40] However, there is evidence that the magnitude of viral shedding in humans may vary for different SARS-CoV-2 variants. One recent study reported differences in the levels of infectious virus detected in nasopharyngeal swabs from individuals infected with different variants of SARS-CoV-2, including Delta and Omicron.[41] Similarly, several studies have reported increased levels of viral RNA in nasal swab samples for more recent variants.[13,17,18,42] Another recent study reported that a small cohort of patients infected with the Alpha variant shed greater levels of viral RNA in the exhaled breath relative to other less-transmissible variants.[3]

The reason for this difference between swab samples collected from NHPs and humans in these studies is unclear but may be at least partially due to differences in the study populations. Studies with NHPs utilized healthy adult animals that developed mild, predominantly asymptomatic disease, whereas human samples were collected from symptomatic patients.

It should be noted that while data from oro- and nasopharyngeal swabs provide some insights into viral shedding dynamics in infected animals, it is unclear how such data translate to the potential for disease transmission. A recent study reported no correlation between viral RNA levels measured in swabs to those measured in exhaled breath samples in COVID-19 patients, suggesting that viral RNA load in nasal swabs may not be an appropriate surrogate for shedding in the exhaled breath during quiet breathing.[2] This result is not surprising, as previous studies utilizing chemical analysis and breathing maneuvers have demonstrated that particles exhaled during quiet breathing originate in the deep lung, and not the upper respiratory tract.[29,43–46] It is known that a fraction of particles emitted from the respiratory tract during speaking or coughing originate from the oral cavity.[29] Thus, the viral load detected in oral swabs or saliva samples may better correlate with the potential for aerosol and/or droplet transmission of disease during speaking or coughing. However, additional studies are needed to better characterize these relationships.

SARS-CoV-2 RNA was detected in five filter samples of the exhaled breath from five different animals—four exposed to the Gamma variant and one exposed to the WA-1 isolate. The emission rates of viral RNA from these animals were between 6 and 7 $\log_{10}$ RNA copies per hour, similar to those reported previously in humans.[4] Unfortunately, a comparison of the levels of viral RNA detected in the exhaled breath to those detected in nasal swabs of NHPs similar to that reported previously for humans[2] was not possible due to the low number of paired positive samples. It should be noted that depressed respiration due to anesthesia has the potential to affect exhaled particle counts, as generation of exhaled particles is known to vary with the degree of respiratory effort.[47,48] Therefore, the particle counts measured in the exhaled breath in the present study are likely lower than would be measured in awake, freely moving animals, and this represents a potential difference that complicates the comparison between exhaled breath data from conscious human patients and anesthetized NHPs.

A previous study reported increases in exhaled particle counts postinfection in NHPs exposed by inhalation to the WA-1 isolate of SARS-CoV-2, as well as a correlation between exhaled particle counts and viral loads measured in nasal swabs by PCR.[31] However, similar relationships were not observed in the present study.[31] The reasons for these differences are unclear, as both studies employed comparable methodologies. In the present study, performance data for the exhaled breath collection system provide confidence that the system provided accurate measurements of particle emission from infected animals. Specifically, the system was operated at a slightly positive pressure to prevent infiltration of ambient particles from the animal holding room, resulting in background particle counts near zero despite the high particle concentration in the room.

Additionally, the median pressure in the mask with an animal present was similar to that observed with the sealed mask (+0.1″ water column), providing an indication that the

seal on the mask was not leaking with an animal present. Finally, while most animals had relatively low particle emission rates, several animals generated significantly higher levels of particles, in some cases due to sneezes or oral movements, demonstrating that higher particle emission rates are detectable in the system.

While the present study reports novel dose–response data for two isolates of SARS-CoV-2, numerous knowledge gaps remain. The present study and others[20,27,31,34] utilize aerosols with aerodynamic diameters in the 1–3 μm range, representative of the size distribution of particles exhaled during quiet breathing.[29,44,46] However, larger particle sizes are possible during other respiratory activities, such as speaking or coughing.[29] Previous studies have demonstrated that particle size alters regional deposition within the respiratory tract, and that deposition patterns within the respiratory tract influence dose–infectivity relationships and disease presentation.[49–53] Therefore, studies examining dose–response relationships for SARS-CoV-2 in larger particle aerosols are needed to more fully understand the hazard posed by aerosol transmission.

Similarly, studies examining the influence of comorbidities, age, and other risk factors on the dose–infectivity relationships for SARS-CoV-2 are needed as epidemiological data suggest that significant differences in morbidity and mortality exist between some groups.[54,55] Finally, while numerous studies have reported the presence of SARS-CoV-2 in the exhaled breath and air samples,[3,4,6–8] data on the magnitude of shedding over time are limited. Therefore, additional studies are needed to better understand shedding dynamics in infected individuals.

Author Disclosure Statement

The authors declare they have no conflicting financial interests.

Funding Information

This work was funded by the National Institute of Allergy and Infectious Disease (NIAID) under Interagency Agreement (IAA) #20056-001 between NIAID and the U.S. Department of Homeland Security Science and Technology Directorate (DHS S&T). Work was performed at the National Biodefense Analysis and Countermeasures Center (NBACC), a Federally Funded Research and Development Center. Funding from NIAID was provided through DHS S&T under Agreement No. HSHQDC-15-C-00064 awarded to Battelle National Biodefense Institute (BNBI) by DHS S&T for the management and operation of the NBACC. This research was supported in part by the Intramural/Extramural research program of the NCATS, NIH. The views and conclusions contained in this document are those of the authors and should not be interpreted as necessarily representing the official policies, either expressed or implied, of DHS, the National Institutes of Health (NIH), or the U.S. Government. The DHS does not endorse any products or commercial services mentioned in this presentation. In no event shall the DHS, BNBI or NBACC have any responsibility or liability for any use, misuse, inability to use, or reliance upon the information contained herein. In addition, no warranty of fitness for a particular purpose, merchantability, accuracy or adequacy is provided regarding the contents of this document. The funders had no role in study design, data collection and analysis, decision to publish, or preparation of the manuscript.

Supplementary Material

Supplementary Data

References

1. Ryan DJ, Toomey S, Madden SF, et al. Use of exhaled breath condensate (EBC) in the diagnosis of SARS-COV-2 (COVID-19). Thorax 2021;76(1):86–88; doi: 10.1136/thoraxjnl-2020-215705
2. Malik M, Kunze A-C, Bahmer T, et al. SARS-CoV-2: Viral loads of exhaled breath and oronasopharyngeal specimens in hospitalized patients with COVID-19. Int J Infect Dis 2021;110:105–110; doi: 10.1016/j.ijid.2021.07.012
3. Adenaiye OO, Lai J, Bueno de Mesquita PJ, et al. Infectious severe acute respiratory syndrome coronavirus 2 (SARS-CoV-2) in exhaled aerosols and efficacy of masks during early mild infection. Clin Infect Dis 2022;75(1): e241–e248; doi: 10.1093/cid/ciab797
4. Ma J, Qi X, Chen H, et al. Coronavirus disease 2019 patients in earlier stages exhaled millions of severe acute respiratory syndrome coronavirus 2 per hour. Clin Infect Dis 2021;72(10):e652–e654; doi: 10.1093/cid/ciaa1283
5. Fox-Lewis A, Williamson F, Harrower J, et al. Airborne transmission of SARS-CoV-2 delta variant within tightly monitored isolation facility, New Zealand (Aotearoa). Emerg Infect Dis 2021;28(3):501–509; doi: 10.3201/eid2803.212318
6. Lednicky JA, Lauzardo M, Alam MM, et al. Isolation of SARS-CoV-2 from the air in a car driven by a COVID patient with mild illness. Int J Infect Dis 2021;108:212–216; doi: 10.1016/j.ijid.2021.04.063
7. Lednicky JA, Lauzardo M, Hugh Fan Z, et al. Viable SARS-CoV-2 in the air of a hospital room with COVID-19 patients. Int J Infect Dis 2020;100:476–482; doi: 10.1016/j.ijid.2020.09.025
8. Santarpia JL, Herrera VL, Rivera DN, et al. The size and culturability of patient-generated SARS-CoV-2 aerosol. J Exposure Sci Environ Epidemiol 2022;32(5):706–711; doi: 10.1038/s41370-021-00376-8
9. Chia PY, Coleman KK, Tan YK, et al. Detection of air and surface contamination by SARS-CoV-2 in hospital rooms of infected patients. Nat Commun 2020;11(1):2800; doi: 10.1038/s41467-020-16670-2
10. Liu Y, Ning Z, Chen Y, et al. Aerodynamic analysis of SARS-CoV-2 in two Wuhan hospitals. Nature 2020; 582(7813):557–560; doi: 10.1038/s41586-020-2271-3
11. Campbell F, Archer B, Laurenson-Schafer H, et al. Increased transmissibility and global spread of SARS-CoV-2 variants of concern as at June 2021. Eurosurveillance 2021; 26(24):2100509; doi: 10.2807/1560-7917.ES.2021.26.24.2100509
12. Davies NG, Abbott S, Barnard RC, et al. Estimated transmissibility and impact of SARS-CoV-2 lineage B. 1.1. 7 in England. Science 2021;372(6538):eabg3055; doi: 10.1126/science.abg3055
13. Moreira FRR, D'arc M, Mariani D, et al. Epidemiological dynamics of SARS-CoV-2 VOC Gamma in Rio de Janeiro, Brazil. Virus Evol 2021;7(2):veab087; doi: 10.1093/ve/veab087
14. Tao K, Tzou PL, Nouhin J, et al. The biological and clinical significance of emerging SARS-CoV-2 variants. Nat Rev Genet 2021;22(12):757–773; doi: 10.1038/s41576-021-00408-x

15. Washington NL, Gangavarapu K, Zeller M, et al. Emergence and rapid transmission of SARS-CoV-2 B. 1.1. 7 in the United States. Cell 2021;184(10):2587.e7–2594.e7; doi: 10.1016/j.cell.2021.03.052
16. Teyssou E, Delagrèverie H, Visseaux B, et al. The Delta SARS-CoV-2 variant has a higher viral load than the Beta and the historical variants in nasopharyngeal samples from newly diagnosed COVID-19 patients. J Infect 2021;83(4): e1–e3; doi: 10.1016/j.jinf.2021.08.027
17. Teyssou E, Soulie C, Visseaux B, et al. The 501Y. V2 SARS-CoV-2 variant has an intermediate viral load between the 501Y. V1 and the historical variants in nasopharyngeal samples from newly diagnosed COVID-19 patients. J Infect 2021;83(4):e1–e3; doi: 10.1016/j.jinf.2021.08.027
18. Bolze A, Luo S, White S, et al. SARS-CoV-2 variant Delta rapidly displaced variant Alpha in the United States and led to higher viral loads. Cell Rep Med 2022;3(3):100564; doi: 10.1016/j.xcrm.2022.100564
19. Li B, Deng A, Li K, et al. Viral infection and transmission in a large, well-traced outbreak caused by the SARS-CoV-2 Delta variant. Nat Commun 2022;13(1):1–9; doi: 10.1038/s41467-022-28089-y
20. Dabisch PA, Biryukov J, Beck K, et al. Seroconversion and fever are dose-dependent in a nonhuman primate model of inhalational COVID-19. PLoS Pathogens 2021;17(8): e1009865; doi: 10.1371/journal.ppat.1009865
21. Ryan KA, Bewley KR, Fotheringham SA, et al. Dose-dependent response to infection with SARS-CoV-2 in the ferret model and evidence of protective immunity. Nat Commun 2021;12(1):18; doi: 10.1038/s41467-020-20439-y
22. Yinda CK, Port JR, Bushmaker T, et al. K18-hACE2 mice develop respiratory disease resembling severe COVID-19. PLoS Pathogens 2021;17(1):e1009195; doi: 10.1371/journal.ppat.1009195
23. Plante JA, Liu Y, Liu J, et al. Spike mutation D614G alters SARS-CoV-2 fitness. Nature 2021;592(7852):116–121; doi: 10.1038/s41586-020-2895-3
24. Bayarri-Olmos R, Jarlhelt I, Johnsen LB, et al. Functional effects of receptor-binding domain mutations of SARS-CoV-2 B. 1.351 and P. 1 variants. Front Immunol 2021;12: 757197; doi: 10.3389/fimmu.2021.757197
25. Escalera A, Gonzalez-Reiche AS, Aslam S, et al. Mutations in SARS-CoV-2 variants of concern link to increased spike cleavage and virus transmission. Cell Host Microbe 2022;30(3):373.e7–387.e7; doi: 10.1016/j.chom.2022.01.006
26. National Research Council. Guide for the Care and Use of Laboratory Animals. National Academies Press: Washington, DC; 2011.
27. Johnston SC, Ricks KM, Jay A, et al. Development of a coronavirus disease 2019 nonhuman primate model using airborne exposure. PLoS One 2021;16(2):e0246366; doi: 10.1371/journal.pone.0246366
28. Bixler SL, Stefan CP, Jay AN, et al. Exposure route influences disease severity in the COVID-19 cynomolgus macaque model. Viruses 2022;14(5):1013; doi: 10.3390/v14051013
29. Johnson G, Morawska L, Ristovski Z, et al. Modality of human expired aerosol size distributions. J Aerosol Sci 2011; 42(12):839–851; doi: 10.1016/j.jaerosci.2011.07.009
30. Payton ME, Greenstone MH, Schenker N. Overlapping confidence intervals or standard error intervals: What do they mean in terms of statistical significance? J Insect Sci 2003;3(1):34; doi: 10.1093/jis/3.1.34
31. Edwards DA, Ausiello D, Salzman J, et al. Exhaled aerosol increases with COVID-19 infection, age, and obesity. Proc Natl Acad Sci USA 2021;118(8):e2021830118; doi: 10.1073/pnas.2021830118
32. Bielecki M, Züst R, Siegrist D, et al. Social distancing alters the clinical course of COVID-19 in young adults: A comparative cohort study. Clin Infect Dis 2021;72(4):598–603; doi: 10.1093/cid/ciaa889
33. Guallar MP, Meiriño R, Donat-Vargas C, et al. Inoculum at the time of SARS-CoV-2 exposure and risk of disease severity. Int J Infect Dis 2020;97:290–292; doi: 10.1016/j.ijid.2020.06.035
34. Hartman AL, Nambulli S, McMillen CM, et al. SARS-CoV-2 infection of African green monkeys results in mild respiratory disease discernible by PET/CT imaging and shedding of infectious virus from both respiratory and gastrointestinal tracts. PLoS Pathogens 2020;16(9):e1008903; doi: 10.1371/journal.ppat.1008903
35. Liu J, Li H, Luo M, et al. Lymphopenia predicted illness severity and recovery in patients with COVID-19: A single-center, retrospective study. PLoS One 2020;15(11): e0241659; doi: 10.1371/journal.pone.0241659
36. Liu F, Li L, Xu M, et al. Prognostic value of interleukin-6, C-reactive protein, and procalcitonin in patients with COVID-19. J Clin Virol 2020;127:104370; doi: 10.13039/501100001809
37. Kong M, Zhang H, Cao X, et al. Higher level of neutrophil-to-lymphocyte is associated with severe COVID-19. Epidemiol Infect 2020;148:e139; doi: 10.1017/S0950268820001557
38. Liu J, Liu Y, Xiang P, et al. Neutrophil-to-lymphocyte ratio predicts critical illness patients with 2019 coronavirus disease in the early stage. J Transl Med 2020;18(1):206; doi: 10.1186/s12967-020-02374-0
39. Asakura H, Ogawa H. COVID-19-associated coagulopathy and disseminated intravascular coagulation. Int J Hematol 2021;113(1):45–57; doi: 10.1007/s12185-020-03029-y
40. Munster V, Flagg M, Singh M, et al. Subtle differences in the pathogenicity of SARS-CoV-2 variants of concern B. 1.1. 7 and B. 1.351 in rhesus macaques. bioRxiv; 2021.
41. Puhach O, Adea K, Hulo N, et al. Infectious viral load in unvaccinated and vaccinated individuals infected with ancestral, Delta or Omicron SARS-CoV-2. Nat Med 2022;28(7):1491–1500; doi: 10.1038/s41591-022-01816-0
42. Lu J, Li B, Deng A, et al. Viral infection and transmission in a large, well-traced outbreak caused by the SARS-CoV-2 Delta variant. Nat Commun 2022;13(1):460; doi: 10.1038/s41467-022-28089-y
43. Johnson GR, Morawska L. The mechanism of breath aerosol formation. J Aerosol Med Pulm Drug Deliv 2009; 22(3):229–237; doi: 10.1089/jamp.2008.0720
44. Morawska L, Johnson G, Ristovski Z, et al. Size distribution and sites of origin of droplets expelled from the human respiratory tract during expiratory activities. J Aerosol Sci 2009;40(3):256–269; 10.1016/j.jaerosci.2008.11.002
45. Bredberg A, Gobom J, Almstrand A-C, et al. Exhaled endogenous particles contain lung proteins. Clin Chem 2012; 58(2):431–440; doi: 10.1373/clinchem.2011.169235
46. Scheuch G. Breathing is enough: For the spread of influenza virus and SARS-CoV-2 by breathing only. J Aerosol Med Pulm Drug Deliv 2020;33(4):230–234; doi: 10.1089/jamp.2020.1616

47. Wilson N, Marks G, Eckhardt A, et al. The effect of respiratory activity, non-invasive respiratory support and facemasks on aerosol generation and its relevance to COVID-19. Anaesthesia 2021;76(11):1465–1474; doi: 10.1111/anae.15475
48. Fairchild C, Stampfer J. Particle concentration in exhaled breath. Am Industr Hygiene Assoc J 1987;48(11):948–949; doi: 10.1080/15298668791385868
49. Dabisch PA, Xu Z, Boydston JA, et al. Quantification of regional aerosol deposition patterns as a function of aerodynamic particle size in rhesus macaques using PET/CT imaging. Inhalat Toxicol 2017;29(11):506–515; doi: 10.1080/08958378.2017.1409848
50. Sonkin LS. Infections induced in mice by local application of streptococci and pneumococci to the nasal mucosa and by intrapulmonary instillation. J Infect Dis 1949;84(3):290–305; doi: 10.1093/infdis/84.3.290
51. Wells WF. Airborne Contagion and Air Hygiene: An Ecological Study of Droplet Infections. JAMA 1955;159(1):90; doi: 10.1001/jama.1955.02960180092033
52. Fitzgeorge R, Baskerville A, Broster M, et al. Aerosol infection of animals with strains of Legionella pneumophila of different virulence: Comparison with intraperitoneal and intranasal routes of infection. Epidemiol Infect 1983;90(1):81–89; doi: 10.1017/s0022172400063877
53. Sonkin LS. The role of particle size in experimental airborne infection. Am J Hygiene 1951;53(3):337–354; doi: 10.1093/oxfordjournals.aje.a119459
54. Tsankov BK, Allaire JM, Irvine MA, et al. Severe COVID-19 infection and pediatric comorbidities: A systematic review and meta-analysis. Int J Infect Dis 2021;103:246–256; doi: 10.1016/j.ijid.2020.11.163
55. Thakur B, Dubey P, Benitez J, et al. A systematic review and meta-analysis of geographic differences in comorbidities and associated severity and mortality among individuals with COVID-19. Sci Rep 2021;11(1):8562; doi: 10.1038/s41598-021-88130-w

Received on June 27, 2022
in final form, August 20, 2022

Reviewed by:
Philip Kuehl and Margaret Pitt

Address correspondence to:
Paul A. Dabisch, PhD
National Biodefense Analysis
and Countermeasures Center
Operated by Battelle National Biodefense Institute
for the U.S. Department of Homeland Security
8300 Research Plaza
Frederick, MD 21701
USA

E-mail: paul.dabisch@nbacc.dhs.gov